

---

# Directly Optimizing Explanations for Desired Properties

---

Hiwot Belay Tadesse  
Harvard University

Alihan Hüyük  
Harvard University

Weiwei Pan  
Harvard University

Finale Doshi-Velez  
Harvard University

## Abstract

When explaining black-box machine learning models, it’s often important for explanations to have certain desirable properties. Most existing methods ‘encourage’ desirable properties in their construction of explanations. In this work, we demonstrate that these forms of encouragement do not consistently create explanations with the properties that are supposedly being targeted. Moreover, they do not allow for any control over which properties are prioritized when different properties are at odds with each other. We propose to *directly optimize* explanations for desired properties. Our direct approach not only produces explanations with optimal properties more consistently but also empowers users to control trade-offs between different properties, allowing them to create explanations with exactly what is needed for a particular task.

## 1 INTRODUCTION

When trying to explain black-box machine learning models to humans, it is often important for our explanations to have certain desirable mathematical *properties*. In fact, an growing body of works show humans find different explanations properties useful for different tasks (Zhou et al., 2021; Liao et al., 2022; Nofshin et al., 2024). For example, studies show that, when auditing black-box models for compliance, humans may prefer *faithful* explanations, where the explanations accurately reflect the actual computations carried out by the underlying model; when performing counter-factual (“what-if”) reasoning about black-box models, humans may prefer *robust* explanations, where similar inputs are assigned similar explanations Nofshin et al. (2024). Other studies show that when trying to detect model biases human may prefer *smooth* explanations, where

similar dimensions in the input are assigned similar values in the explanation Colin et al. (2022). As user studies provide a clearer picture of which explanation properties are needed for which tasks, we have a corresponding computational need to be able to produce explanations that can achieve these properties.

In this work, we focus on feature attribution explanations – explanations that assign a contribution score (possibly negative) to capture the impact of each input dimension on the output. There are a large number of feature attribution methods (e.g. Ribeiro et al., 2016; Lundberg and Lee, 2017; Smilkov et al., 2017; Selvaraju et al., 2020), some of which specifically encourage explanations to have certain properties. For example, SmoothGrad (Smilkov et al., 2017) aims to encourage robustness by averaging gradients around the input. Meanwhile, LIME (Ribeiro et al., 2016) prioritizes faithfulness by fitting a linear model near the input.

However, even though current feature attribution methods try to encourage for a particular property when constructing explanations, they do not directly optimize explanations for properties. Thus, these methods may not reliably produce explanations with the targeted property across different machine learning models or across different parts of the input space for the same model. Moreover, most explanation properties (e.g. faithfulness) have many different mathematical formalizations (Chen et al., 2022). Just because a feature attribution method produces explanations that scores well under one property formalization, it may not score well under another. This is a problem when a downstream task calls for an explanation that satisfies a specific formalization of a property. Finally, additional challenges arise when one needs an explanation that satisfies multiple properties. Often, properties can be in tension with each other (Tan and Tian, 2023b), meaning that explanations that have more of one property may have less of another. Therefore, finding explanations that satisfy multiple properties will require carefully managing trade-offs between them.

In this work, we argue for the need to *directly* optimize explanations for desired properties. We derive computationally efficient ways to perform this optimization,

arXiv:2410.23880v1 [cs.LG] 31 Oct 2024

while allowing us to intuitively trade-off between a range of common properties in both inductive and transductive settings. In the inductive setting, we show that optimizing an additive combination of faithfulness, robustness, and smoothness is equivalent to a Gaussian process (GP) inference problem, and can be solved with theoretical guarantees using GP methods. While the inductive setting is general and theoretically grounded, the transductive setting allows us to consider an even wider range of properties and efficient optimization regimes. In particular, in the transductive setting, we consider optimizing for complexity and alternative formulations of robustness and faithfulness from the literature.

**Contributions.** We make three contributions: (1) Rather than implicitly encouraging desired properties, we explicitly optimize for these properties and develop efficient methods for such optimizations. (2) We demonstrate that popular feature attribution methods (e.g. SmoothGrad, LIME, SHAP) not only fail to reliably find explanations with optimal properties, they also do not allow for control over prioritization of properties. (3) Finally, we show that our approach yields explanations with optimal properties more consistently than baselines. Moreover, our approach allows for fine-grained control over the trade-offs between competing properties. This control allows us to create feature attribution explanations with exactly the balance of properties that is needed for a particular task.

## 2 RELATED WORK

### Limitations of Current Explanation Methods.

Many feature attribution methods in the literature aim to produce explanations with certain properties. However, none of these methods explicitly optimize explanations for desirable properties. As a consequence, depending on their hyper-parameters, these methods may fail to produce optimal explanations with respect to their target properties; or, they make implicit and unpredictable trade-offs between properties. For example, Alvarez-Melis and Jaakkola (2018); Ghorbani et al. (2018); Slack et al. (2020) showed that explanations generated by LIME (Ribeiro et al., 2016) and SHAP (Lundberg and Lee, 2017), which encourage explanation faithfulness, are not always robust. On the other hand, Adebayo et al. (2018) showed that explanations generated by SmoothGrad Smilkov et al. (2017) and GradCAM Selvaraju et al. (2020), which encourage explanation robustness, may lack faithfulness.

**Tensions between Explanation Properties.** While sometimes there can be synergies between the different properties (Yeh et al., 2019b); but more often they are in tension: prior works have analyzed tensions between faithfulness and complexity (Bhatt et al., 2020),

faithfulness and sensitivity Bansal et al. (2020), and homogeneity and faithfulness (Balagopalan et al., 2022). Without explicit optimization, existing methods do not provide sufficient transparency in managing tensions between different properties. For instance, Tan and Tian (2023b) demonstrated that a trade-off exists between faithfulness and robustness for explanations generated by SmoothGrad that is sensitive to its main hyperparameter  $\delta$ . However, how exactly  $\delta$  affects this trade-off remains unclear (we will show in the experiments that varying  $\delta$  can lead to unintuitive changes in faithfulness and robustness). To address this problem, (Cugny et al., 2022) proposed a framework for recommending explanations based on the user’s specific needs and constraints. However, their work relies on adapting hyperparameters of existing explanation methods, which may not cover the full space of explanations and thus miss ones that produce the most optimal trade-off.

### Directly Optimizing Explanations for Properties.

Recently, (Bhatt et al., 2020; Decker et al., 2024) proposed linearly aggregating explanations generated from different explanation methods to obtain explanations with more optimal properties. This work is closest to ours in that it performs direct optimization on explanation. However, the optimality of the final explanation generated by this approach is limited by the the linear span of the initial set of explanations. Furthermore, this approach does not address the need for *consistency* across explanations for multiple inputs. Our direct optimization approach addresses these concerns, as well as provides an efficient way to tune one’s priorities over different explanation properties.

## 3 PROBLEM FORMULATION

**Settings.** We consider the problem of explaining some fixed function  $f : \mathbb{R}^D \rightarrow \mathbb{R}$ . We assume that we can query the function for an output  $y = f(\mathbf{x})$  for any input  $\mathbf{x}$  as well as a gradient  $\nabla f(\mathbf{x})$ . Depending on how explanations are requested, we consider two different settings: (i) the *inductive setting*, where the requests for explanations arrive in an online fashion (i.e. one input point  $\mathbf{x}^*$  at a time), and (ii) the *transductive setting*, where we are given the full set of input points  $\{\mathbf{x}_n\}_{n=1}^N$  that we will need to explain in advance. While the inductive setting is more generally applicable, it is also a more challenging setting; the assumption of the transductive setting will allow us to optimize for a wider range of properties than the inductive setting.

**Explanations.** In this paper, we restrict our focus to local explanations that are based on feature-attributions. This is so that we can give concrete definitions of properties such as faithfulness, robustness, and smoothness as an exemplar of our approach. We emphasize that the idea of *optimizing explanations*

for desired properties remains general. In local feature attribution, an explanation  $\mathbf{E} \in \mathbb{R}^D$  is a vector assigning an attribution score to each component of some input point  $\mathbf{x}$ . In the inductive settings, these explanations are given by a function  $E : \mathbb{R}^D \rightarrow \mathbb{R}^D$ . In the transductive setting, we do not assume an explicit explanation function, rather, for each input  $\mathbf{x}_n$ , we denote the explanation at  $\mathbf{x}_n$  by  $\mathbf{w}_{E_n} \in \mathbb{R}^D$  and the matrix of explanations for the  $N$  inputs as  $W_E \in \mathbb{R}^{N \times D}$ .

**The General Problem.** Fix a set of desired properties  $\{\text{prop}_i\}$ , each characterized by a loss function  $\mathcal{L}_{\text{prop}_i}$ . In the inductive setting, these losses are functions of  $E$ , and in the transductive setting, they are functions of  $W_E$ . Our objective is to find the explanation function  $E$ —or the explanation matrix  $W_E$ —that optimizes for the given properties (i.e. minimizes their characteristic loss functions):

$$E^* = \operatorname{argmin}_E \sum_i \lambda_{\text{prop}_i} \mathcal{L}_{\text{prop}_i}(E; f) \quad (1)$$

where  $\lambda_{\text{prop}_i}$  are importance weights. These weights provide a transparent, intuitive way to manage trade-offs between different properties in the optimization.

**Property Definitions.** In this paper, we optimize for a range of common properties that have been shown to be useful for downstream tasks in literature. In existing literature, the same conceptual property is mathematically formalized in many different ways (Chen et al., 2022) (e.g. Alvarez Melis and Jaakkola (2018b) vs. Yeh et al. (2019b) for robustness). We focus on the properties of faithfulness, robustness, smoothness and complexity; and we choose formalizations of these properties that have been well studied in literature, as well as lend themselves to efficient optimization.

**Faithfulness.** Faithfulness quantifies the extent to which an explanation accurately reflect the behavior of the function it is explaining. The class of explanations wherein one computes the marginal contribution of each dimension, by using small perturbations or by analytically computing input gradients, can be seen as optimizing faithfulness formalized as gradient matching (Baehrens et al., 2010; Simonyan, 2013):

$$\mathcal{L}_{\text{faithful}}(E) = \int_{\Omega} \|E(\mathbf{x}) - \nabla f(\mathbf{x})\|_2^2 d\mathbf{x} \quad (2)$$

where  $\Omega$  is the domain of function  $f$ . In the transductive setting, this becomes  $\mathcal{L}_{\text{faithful}}(W_E) = \sum_{n=1}^N \|\mathbf{w}_{E_n} - \nabla f(\mathbf{x}_n)\|_2^2$ . Many faithfulness metrics proposed in the literature can be reduced to gradient matching under certain settings. For example, the faithfulness metric proposed in Tan and Tian (2023a) is equivalent to gradient matching, when the perturbation is Gaussian and the similarity measure is Euclidean distance.

**Robustness.** Robustness quantifies the extent to which an explanation varies with respect to the input.

A common way to formalize robustness as a metric is to take the weighted sum of pairwise differences between explanations for different inputs in the data. More formally, in the inductive setting, this can be written:

$$\mathcal{L}_{\text{robust}}(E) = \iint_{\Omega} \|E(\mathbf{x}) - E(\mathbf{x}')\|_2^2 s(\mathbf{x}, \mathbf{x}') d\mathbf{x} d\mathbf{x}' \quad (3)$$

where  $s(\mathbf{x}, \mathbf{x}') \in \mathbb{R}$  is a weight that quantifies the similarity between  $\mathbf{x}$  and  $\mathbf{x}'$ . In the transductive setting, this becomes  $\mathcal{L}_{\text{robust}}(W_E) = \sum_{n,n'} \|\mathbf{w}_{E_n} - \mathbf{w}_{E_{n'}}\|_2^2 S_{nn'}$ , where  $S_{nn'} = s(\mathbf{x}_n, \mathbf{x}_{n'})$  is the matrix of pairwise similarity scores evaluated on  $N$  inputs. Metrics like (Lipschitz) local-stability (Alvarez Melis and Jaakkola, 2018a; Wang et al., 2020) are instances of the above equation, where we set the weights  $S(\mathbf{x}, \mathbf{x}')$  to be a function of  $\|\mathbf{x} - \mathbf{x}'\|_2^2$ . Notably, our robustness loss depends on the similarity of the explanation at input  $\mathbf{x}$  to the explanation at input  $\mathbf{x}'$ . Thus, optimizing the robustness of an explanation for even *one* input requires assigning explanations to *many* other inputs. Our direct optimization approach will ensure that all explanation assignments are consistent, a property not present in existing explanation methods. We detail our choice of  $s$  in the appendix. **Smoothness.** Smoothness or “internal robustness” captures the variability across different dimensions of an explanation that is assigned to a fixed input. Similar to robustness, suppose we are given a similarity matrix  $\tilde{S}_{dd'}$  that tells how similar an input dimension  $d \in [D]$  is to another input dimension  $d' \in [D]$  (for instance, when inputs are images, this similarity can be related to the distance between two pixels). Then, we define the smoothness loss in a form similar to robustness:

$$\mathcal{L}_{\text{smooth}}(E) = \int_{\Omega} \sum_{d,d'} |E_d(\mathbf{x}) - E_{d'}(\mathbf{x})|^2 \tilde{S}_{dd'} \quad (4)$$

in the inductive setting, which can be expressed as  $\mathcal{L}_{\text{smooth}}(W_E) = \sum_{n,d,d'} |(\mathbf{w}_{E_n})_d - (\mathbf{w}_{E_n})_{d'}|^2 \tilde{S}_{dd'}$  in the transductive setting.

## 4 INDUCTION: OPTIMIZING EXPLANATION FUNCTIONS

In this section, we tackle the inductive version of our problem: learning explanation functions that are optimized for a set of desired explanation properties. We instantiate the general problem in Equation 1 with three properties  $\{\text{faithful}, \text{robust}, \text{smooth}\}$ . Then, we drive a computationally efficient and mathematically consistent solution based on GP inference.

**The Inductive Problem.** We observe that the definitions of faithfulness, robustness, and smoothness from Section 3 are quadratic. When linearly combined, these losses lead to the following optimization problem

(setting  $\lambda_{\text{faithful}} = 1$  without a loss of generality):

$$\begin{aligned} E^* &= \operatorname{argmin}_E \int_{\Omega} \|E(\mathbf{x}) - \nabla f(\mathbf{x})\|_2^2 d\mathbf{x} \\ &+ \lambda_{\text{robust}} \iint_{\Omega} \|E(\mathbf{x}) - E(\mathbf{x}')\|_2^2 s(\mathbf{x}, \mathbf{x}') d\mathbf{x} d\mathbf{x}' \quad (5) \\ &+ \lambda_{\text{smooth}} \int_{\Omega} \sum_{d,d'} |E_d(\mathbf{x}) - E_{d'}(\mathbf{x})|^2 \tilde{S}_{dd'} d\mathbf{x} \end{aligned}$$

While the most general form of Equation 1 may be difficult to solve, below we derive how the optimization in Equation 5 can be cast as a very specific kind of GP regression—and that will yield a both computationally tractable and mathematically consistent solution.

### Equivalence to Gaussian Process Regression.

The robustness loss in Equation 5 is what makes optimization challenging: when assigning an explanation even to one input, we must ensure that the explanation is similar to explanations for nearby inputs; those explanations, to be optimal, must in turn also be faithful, robust, and smooth. To get a consistent solution, we must reason in the space of explanation functions  $E(\mathbf{x})$ .

Gaussian process (GP) regression provides a theoretically grounded and computationally tractable framework for inference in function space. Below we show that the solution to the optimization problem in Equation 5 is the maximum a posteriori function of a multi-output Gaussian process, in which the ground-truth explanations  $\nabla f$  can be interpreted as the likelihood term, the  $s, \tilde{S}$  can be written as the inverse of a multi-output kernel, and where we marginalize over an unknown mean explanation value parameter. Viewed as GP regression, we can derive a consistent, analytic solution to Equation 5 for any number of query points.

Formally, let us start with the following GP prior in which the ground-truth explanations are interpreted as the observations of the latent explanation function:

$$\begin{aligned} E &\sim \text{GP}(m, K), \quad m(\mathbf{x}) = \mu \mathbf{1}_D, \\ \mu &\sim \mathcal{N}(0, \sigma^2), \quad \nabla f(\mathbf{x}) \sim \mathcal{N}(E(\mathbf{x}), I) \end{aligned} \quad (6)$$

where  $\mu$  represents the unknown mean explanation value (identical for all inputs and all dimensions) and the kernel  $K$  is a matrix-valued function such that  $\text{cov}(E_d(\mathbf{x}), E_{d'}(\mathbf{x}')) = K_{dd'}(\mathbf{x}, \mathbf{x}')$  with its inverse denoted as  $K^{-1}$ . Then, we have the following equivalence:

**Proposition 1.** *For  $\{\mathbf{x}_n\}_{n=1}^N$  and  $\mathbf{x}_n \sim \text{Uniform}(\Omega)$ , the maximum a posteriori function*

$$\operatorname{argmax}_E p(E|\{\mathbf{x}_n, \nabla f(\mathbf{x}_n)\}) \quad (7)$$

*approaches to the optimal explanation function*

$$\begin{aligned} \operatorname{argmin}_E \int_{\Omega} \|E(\mathbf{x}) - \nabla f(\mathbf{x})\|_2^2 \\ - \iint_{\Omega} \sum_{dd'} |E_d(\mathbf{x}) - E_{d'}(\mathbf{x}')|^2 K_{dd'}^{-1}(\mathbf{x}, \mathbf{x}') d\mathbf{x} d\mathbf{x}' \end{aligned} \quad (8)$$

as  $\sigma^2 \rightarrow \infty$  and  $N \rightarrow \infty$ .

*Proof.* The complete proof can be found in the appendix. However, the key insight is to write the inductive optimization in Equation 8 as the limiting case of a transductive optimization, which allows us to manipulate it algebraically to show its equivalence to the inference problem in Equation 7.  $\square$

When the similarity measures in Equation 5 are precision functions corresponding to kernels, that is  $s(\mathbf{x}, \mathbf{x}') = -k_{\text{robust}}^{-1}(\mathbf{x}, \mathbf{x}')$  and  $\tilde{S} = -K_{\text{smooth}}^{-1}$ , we can define the GP kernel  $K$  in Equation 6 such that

$$\begin{aligned} K_{dd'}^{-1}(\mathbf{x}, \mathbf{x}') &= \lambda_{\text{robust}} \cdot k_{\text{robust}}^{-1} \cdot \mathbb{1}\{d = d'\} \\ &+ \lambda_{\text{smooth}} \cdot \mathbb{1}\{\mathbf{x} = \mathbf{x}'\} \cdot (K_{\text{smooth}}^{-1})_{dd'} \end{aligned} \quad (9)$$

Then, the objective in the proposition (Equation 8) becomes equivalent to the objective in our explanation property optimization problem (Equation 5). Thus, the solution to our optimization problem can be computed via GP inference (via Proposition 1); in particular, we can find efficient solutions to our optimization problem through approximate GP inference. Concretely, we can select a set of *inducing points*  $\{\mathbf{x}_n\}$  to approximately perform GP inference. In our experiments, we investigate the sensitivity of our approach to selection of inducing points (particularly its size  $N$ ).

## 5 TRANSDUCTION: OPTIMIZING EXPLANATIONS ON FIXED SETS

Optimization in the inductive setting is generally challenging because the explanation function must be consistent across all possible inputs. In this section, we describe how optimization can be made even more efficient in the transductive setting, where we have, in advance, a fixed set of inputs  $\mathbf{x}_n$  that we want to explain. In particular, we identify specific classes of properties for which the optimization problem in the transductive setting can be solved analytically or efficiently and with guarantees, i.e. by recasting these problems as linear or quadratic programs.

**Connecting to the Inductive Setting.** When we instantiate Equation 1 using the definitions of faithfulness, robustness, and smoothness from Section 3, the optimization problem defines a quadratic program:

$$\begin{aligned} W^* &= \operatorname{argmin}_{W_E} \lambda_{\text{faithful}} \sum_n \|\mathbf{w}_{E_n} - \nabla f(\mathbf{x}_n)\|_2^2 \\ &+ \lambda_{\text{robust}} \sum_{n,n'} \|\mathbf{w}_{E_n} - \mathbf{w}_{E_{n'}}\|_2^2 S_{nn'} \quad (10) \\ &+ \lambda_{\text{smooth}} \sum_{n,d,d'} |(\mathbf{w}_{E_n})_d - (\mathbf{w}_{E_{n'}})_{d'}|^2 \tilde{S}_{dd'} \end{aligned}$$

where  $S_{nn'}$  captures a notion of similarity between the inputs  $\mathbf{x}_n$  and  $\mathbf{x}_{n'}$ , and  $\tilde{S}_{dd'}$  captures a notion of similarity between the input dimensions  $d$  and  $d'$ .

Furthermore, we note that when we choose  $S$  and  $\tilde{S}$  to be the negative precision matrices for kernels  $K$  and  $\tilde{K}$ , we can still take advantage of Proposition 1 (when  $N$  is large!) and use GP inference to find a solution. Doing so, the faithfulness objective follows from the Gaussian likelihood and the robustness objective is determined by our choice of kernel in the prior. This connection to GP inference provides theoretical grounding for the multi-property optimization problem in Equation 1.

**The Transductive Problem.** For the transductive setting, we are able to introduce a fourth property: *complexity*. We focus on an instance of the multi-property optimization problem in Equation 1 where we trade off between complexity and our previous properties, faithfulness, robustness, and smoothness, and where direct global optimization can be made efficient by our choices of the forms of these four properties:

$$W^* = \operatorname{argmin}_{W_E} \lambda_{\text{faithful}} \mathcal{L}_{\text{faithful}}(W_E) + \lambda_{\text{robust}} \mathcal{L}_{\text{robust}}(W_E) + \lambda_{\text{smooth}} \mathcal{L}_{\text{smooth}}(W_E) + \lambda_{\text{complex}} \mathcal{L}_{\text{complex}}(W_E) \quad (11)$$

We choose to work with these four properties because they are in tension—that is, it is not possible to maximize all four unless the function has constant gradients (i.e. it is linear). Thus, it is necessary for any explanation method to manage the trade-off between faithfulness, robustness, smoothness, and complexity in ways that are appropriate for specific tasks.

**Efficient Optimization.** In the transductive setting, we have the ability to efficiently optimize a large number of additional formalizations of properties by recasting them as quadratic or linear programs. In particular, we will consider one additional formalization of faithfulness (*function matching*), one additional formalization of robustness (*maximum difference*) and a formalization of complexity (*sparsity*). In this paper we do not derive instantiations of Equation 11 using these alternate formalizations of properties from the framework of GP regression. However, it would be interesting future work to consider kernels in the inductive setting such that they yield optimization problems in the transductive setting with different formalization of properties.

*Faithfulness as function matching.* A number of metrics define faithfulness as matching the function with linear approximations based on the explanation, e.g. local-fidelity (Yeh et al., 2019a), local-accuracy (Tan and Tian, 2023a), loss-based-fidelity (Balagopalan et al., 2022). Optimizing these metrics can also be recast as an unconstrained quadratic program:

$$W^* = \operatorname{argmin}_{W_E} \underbrace{\sum_n \|f(\mathbf{x}_n) - (\mathbf{w}_{E_n})^\top \mathbf{x}_n\|_2^2}_{\mathcal{L}'_{\text{faithful}}(W_E)} \quad (12)$$

where the explanation at  $\mathbf{x}_n$  are the weights of a linear model approximating the function’s output at  $\mathbf{x}_n$ .

*Robustness as maximum difference.* Metrics like maximum-sensitivity Yeh et al. (2019a) capture a notion of robustness defined by the maximum difference between the explanations at “neighbouring” inputs, that is

$$W^* = \operatorname{argmin}_{W_E} \underbrace{\max_n \|\mathbf{w}_{E_n} - \mathbf{w}_{E_{n'}}\|_2^2}_{\mathcal{L}'_{\text{robust}}(W_E)} \quad (13)$$

Optimizing these metrics can be recast as a linear program with quadratic constraints: minimize  $\sum_n d_n$  subject to  $d_n \geq \|\mathbf{w}_{E_n} - \mathbf{w}_{E_{n'}}\|_2^2$  for all  $n, n'$ .

*Complexity as sparsity.* A common way to formalize explanation complexity is via sparsity, i.e. by counting the number of non-zero weights in the explanation. This metric defines an unconstrained  $\ell_1$  optimization:

$$W^* = \operatorname{argmin}_{W_E} \underbrace{\sum_n \|\mathbf{w}_{E_n}\|_1}_{\mathcal{L}_{\text{complex}}(W_E)} \quad (14)$$

which can be rewritten as a quadratic program and efficiently solved via sequential quadratic programs when integrated with other objectives Schmidt (2005).

In Section 7, for a range of functions, we show that the trade-off hyperparameters  $\{\lambda_{\text{faithful}}, \lambda_{\text{robust}}, \lambda_{\text{smooth}}, \lambda_{\text{complex}}\}$  of our method allow us to explicitly and flexibly prioritize their corresponding properties differently, while baseline like SmoothGrad, LIME and SHAP can only do so in limited ways (if at all). We also explore whether or not insights from our analyses generalize across different choices of the same property.

## 6 EXPERIMENT SETUP

**Inductive Setting.** We show that we can solve the optimization problem in the inductive setting efficiently by using inducing points (i.e. selecting a small subset of the input over which to perform GP inference). Specifically, we check that the explanations generated for a test set in the inductive setting (based on a separate set of inducing points) approach those that could have been generated in the transductive setting, if the test points were available ahead of time. We only consider Gaussian kernels in the inductive setting.

**Transductive Setting.** We compare the explanations generated by our method with baseline feature attribution methods. In particular, we are interested in seeing which methods are able to consistently generate explanations with more optimal properties, and we want to see the extent to which each method allow us to control the trade-offs between different properties. Moreover, we want to compare our method against baselines across a range of function classes, and for multiple formalizations of the same properties.

**Baseline Explanation Methods.** We compare our property-optimized explanations to three popular baselines: SmoothGrad, LIME, and SHAP.

SmoothGrad is defined by averaging gradients of  $f$  over a set of points sampled from a neighbourhood of  $\mathbf{x}_n$ :

$$W_{\text{SG}_n} = \frac{1}{S} \sum_{s=1}^S \nabla f(\tilde{\mathbf{x}}_{n,s}), \quad \tilde{\mathbf{x}}_{n,s} \sim p_{\delta_{\text{SG}}}(\tilde{\mathbf{x}}) \quad (15)$$

where the sampling hyperparameter  $\delta_{\text{SG}}$  controls the size of the neighbourhood. Intuitively,  $\delta_{\text{SG}}$  also controls the degree of smoothing applied to  $W_{\text{SG},n}$ .

LIME approximates  $f$  at  $\mathbf{x}_n$  with a linear model trained on points sampled from a  $\delta_{\text{LIME}}$ -neighbourhood of  $\mathbf{x}_n$ :

$$W_{\text{LIME}_n} = \underset{\mathbf{w}}{\operatorname{argmin}} \sum_{s=1}^S (f(\tilde{\mathbf{x}}_{n,s}) - g(\tilde{\mathbf{x}}_{n,s}, \mathbf{w}))^2 \quad (16)$$

where  $g$  is a weighted linear model  $g(\tilde{\mathbf{x}}_{n,s}, \mathbf{w}) = \mathbf{w}^T \tilde{\mathbf{x}}_{n,s}$ . The sampling hyperparameter  $\delta_{\text{LIME}}$  controls the size of the neighbourhood.

**Functions Classes.** The nature of trade-offs between explanation properties will depend on the underlying function. We consider a number of functions with different degrees of curvature, periodicity/quasi-periodicity.

*Power and Polynomial functions:* We consider functions of the form  $\sum_{d=1}^D (\mathbf{x}^{(d)})^K$ , where  $K$  is a positive integer. We vary the degree  $K$ . We also consider polynomials  $\sum_{d=1}^D (\mathbf{x}^{(d)})^2 + \sum_{d=1}^D \sum_{d'=1}^D \mathbf{x}^{(d)} \mathbf{x}^{(d')}$ .

*Periodic and quasi-periodic functions:* We consider periodic functions of the form  $\sum_{d=1}^D \sin(\mathbf{x}^{(d)})$ . We consider quasi-periodic functions of the forms  $\sum_{d=1}^D \sin e^{\mathbf{x}^{(d)}}$ ,  $\sum_{d=1}^D \mathbf{x}^{(d)} + \sin e^{\mathbf{x}^{(d)}}$  and  $\sum_{d=1}^D (\mathbf{x}^{(d)})^2 / 10 + \sin(3\mathbf{x}^{(d)})$ .

For transductive experiments, we choose  $N = 100^D$  points from a  $D$ -dimensional grid with values in  $(-5, 5)$  for each dimension. For inductive experiments, we set  $D = 3$ , we sample 1000 test points (up to  $N = 1000$  inducing points for GP inference) from the same range.

*Multi-layer perceptrons (MLPs):* We consider neural network models with two hidden layers. We used four datasets from UCI Machine Learning Repository.

*Convolutional neural networks (CNNs):* We consider the model architecture ResNet-50 (He et al., 2016), pretrained on the dataset ImageNet-1k (Russakovsky et al., 2015). For quantitative results, we sample 1000 test images from ImageNet-1k and up to  $N = 1000$  separate images to be used as inducing points. Note that, for these images,  $D = 244 \times 244$ .

**Quantitative Evaluation.** For the inductive setting, we optimize for faithfulness and robustness, fixing  $\lambda_{\text{faithful}} = 1$  and varying  $\lambda_{\text{robust}}$ . We report the total

loss as we vary the number of inducing points  $N$  that are used for GP inference, comparing this with the total loss achievable transductively.

For the transductive setting, we report the individual property-specific losses (e.g. faithfulness) for each explanation method and a wide range of hyperparameters. We report the lowest total loss achieved by each method (over all properties considered) as well as the trade-off each method makes between the different property-specific losses as we vary the hyperparameters (e.g. sampling hyperparameter for LIME and SmoothGrad, trade-off hyperparameters for our method).

**Qualitative Evaluation.** In order to visually highlight the control over different properties provided by our approach, we pick a single image (another examples is in the appendix) from ImageNet-1k and compare the explanations generated for this images by our approach vs. SmoothGrad. Using our approach, we optimize for faithfulness, robustness, and smoothness via GP inference, using perturbations of the original image as inducing points (uniform perturbations as opposed to Gaussian perturbations). We fix  $\lambda_{\text{faithful}} = 1$  and vary  $\lambda_{\text{robust}}$  and  $\lambda_{\text{smooth}}$ . For SmoothGrad, we can only vary  $\delta$  (using Gaussian perturbations to match the Gaussian kernel in our approach). We see that varying  $\delta$  only controls robustness and completely misses smoothness, which happens to be the method’s namesake property.

## 7 RESULTS & ANALYSIS

In this section, we show the quantitative and qualitative comparisons of our method against baselines. We first focus on the transductive setting; highlight the failure modes of baseline explanation methods like LIME and SmoothGrad; demonstrate how our method can directly optimize for desired properties and manage the trade-off between properties that are in tension; and show how different formalizations of a property can be used in our method while still providing similar explanations across these formalizations. Afterwards, we show that inductive solutions can approximate transductive solutions with enough inducing points (albeit more limited in terms of the choice of properties).

**Transductive Setting.** We consider settings when the set of inputs that we want to explain is fixed a priori.

*Intuitive Interpretations of Hyperparameters of SmoothGrad and LIME Can Fail.* A number of works show that  $\delta$ , the sampling hyper-parameter of LIME and SmoothGrad, affect the robustness of these methods. In particular, when the  $\delta$  is larger, LIME and SmoothGrad generate explanations that are less sensitive to local perturbations. However, robustness in these analyses is formalized as local-Lipschitzness, and it is not clear how their insights generalize to other formaliza-

tions. In Figure 1a, we show that, for cubic functions, the robustness (defined in Equation 3) of SmoothGrad does not depend on  $\delta$ . That is, increasing  $\delta$  does not smooth the explanation. *SmoothGrad and LIME can fail to find robust and faithful explanations in counter-intuitive ways.* SmoothGrad and LIME fail to find robust and faithful explanations for functions with high curvature. For instance, for  $f(\mathbf{x}) = \sum_{d=1}^D (\mathbf{x}^{(d)})^3$ , both methods provide a faithful but not robust explanation despite the variation of the sampling hyperparameter  $\delta$  as shown in Figure 1a. In another function,  $f(\mathbf{x}) = \sum_{d=1}^D \sin(\exp(x_d))$  as shown in Figure 1c, we can see how both SmoothGrad and LIME provide explanations by following a specific trend even when the sampling hyperparameter  $\delta$  varies significantly.

*Directly optimizing explanations for desired properties* We observed that the hyperparameters of these explanation methods, such as  $\delta$  for SmoothGrad, cannot effectively control any specific property of an explanation. As shown in Figure 1a, b, and c SmoothGrad and LIME do not directly optimize for a particular property; rather, they provide solutions that follow a trend.

*Managing Trade-off between Properties:* As discussed above, the explanations provided by SmoothGrad and LIME follow a general trend, making it difficult to manage the trade-offs between properties that are in tension, such as faithfulness and robustness, or faithfulness and complexity. In our method, we control two hyperparameters: the trade-off hyperparameter  $\lambda$  and the sampling hyperparameter  $\delta$ . These allow us to consistently provide explanations that directly optimize for a desired property. For example, if we want a faithful explanation consistently, we can set the trade-off hyperparameter  $\lambda$  to a low value so that it directly optimizes for faithfulness. Conversely, if we want a robust explanation, we can increase the value of  $\lambda$  to optimize for robustness. We demonstrated this in 1 a, b, and c.

In other scenarios, where we are interested in a different set of properties, such as complexity and faithfulness, we can adjust the trade-off hyperparameter,  $\lambda$ , to consistently optimize for complexity, as shown in Figures 2a, b and c. Furthermore, if we prefer an explanation that is less complex but still retains some degree of faithfulness, we can balance the trade-off between complexity and faithfulness, as illustrated in Figures 2 a,b, and c. In contrast, LIME and SmoothGrad only provide explanations that follow a trend, which does not allow for managing the trade-off between complexity and faithfulness. In the same figures, we see that our method can provide explanations with different faithfulness/robustness trade-offs by adjusting the trade-off hyperparameter  $\lambda$ , whereas LIME and SmoothGrad provide explanations that are not optimal and do not offer options to manage the trade-off between faithful-

ness and robustness while considering complexity.

*Transparency and Controllability of  $W_{\text{opt}}^*$ :* In scenarios where  $W_{\text{opt}}^*$  do not provide better explanations (lower Faithfulness and Robustness loss) than LIME and SmoothGrad  $W_{\text{opt}}^*$  still manage to match the faithfulness and robustness losses of LIME and SmoothGrad. As shown in Figure 3 d,e, and f  $W_{\text{opt}}^*$  is consistently providing a range of explanations.

*Consistency of Explanations with Different Property Formalizations:* In our method, we can use any formalization of a property and optimize directly for it. In Figure 3, we use the function matching formalization of faithfulness (Eqn 12). We still manage to provide consistent explanations that are optimal, with the option to manage the trade-off between properties.

In contrast, LIME and SmoothGrad fail to provide consistent explanations with different formalizations of a property—faithfulness in this case. For a cubic function, as shown in 3a, both LIME and SmoothGrad provide explanations that are suboptimal and follow a trend. To highlight the inconsistencies of LIME and SmoothGrad, we zoomed in on the previous figure in 3b and 3d. We observed that, for the cubic function, both LIME and SmoothGrad follow a similar trend to the results using gradient matching faithfulness formalization demonstrated in 2, but are more suboptimal here. However, for the sinusoidal function, as shown in Figure 3c, LIME and SmoothGrad provide explanations that follow a different trend compared to the gradient matching faithfulness formalization demonstrated in 1d. We zoomed in on the figure to show how our method consistently provides optimal explanations in 3d. Additionally, we included the results of a different definition of robustness in the appendix.

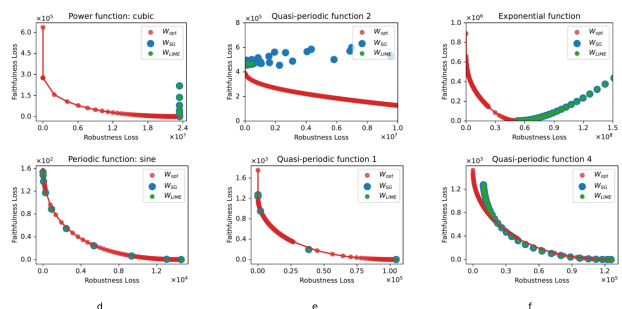


Figure 1: First row: Comparison of Faithfulness and Robustness losses evaluated at  $W_{\text{opt}}$  (RBF Kernel) vs  $W_{\text{SG}}$  and  $W_{\text{LIME}}$  (Normal Sampling). The losses for  $W_{\text{opt}}$  are red,  $W_{\text{SG}}$  are blue and  $W_{\text{LIME}}$  are green. The functions are  $\sum_{d=1}^D x_d^3$ ,  $\sum_{d=1}^D \sin(\exp(x_d))$  and  $\sum_{d=1}^D \exp(x_d)$ . Second row: The Functions are  $\sum_{d=1}^D \sin(x_d)$ ,  $\sum_{d=1}^D (\mathbf{x}^{(d)}) + \sin(3\mathbf{x}^{(d)})$ , and  $\sum_{d=1}^D (\mathbf{x}^{(d)})^2/10 + \sin(3\mathbf{x}^{(d)})$ .

*Comparison with SHAP* we compared our results with

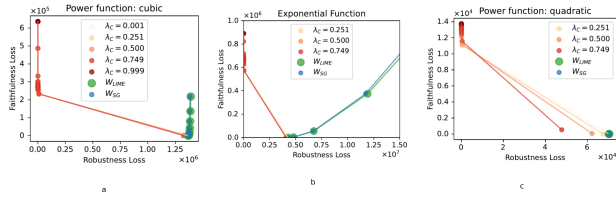


Figure 2: Comparison of  $W_{opt}$  (RBF Kernel) vs  $W_{SG}$  and  $W_{LIME}$  (Normal Sampling). The losses for  $W_{opt}$  are red,  $W_{SG}$  are blue and  $W_{LIME}$  are green. The functions are  $\sum_{d=1}^D x_d^3$ ,  $\sum_{d=1}^D exp(x_d)$  and  $\sum_{d=1}^D x_d^2$

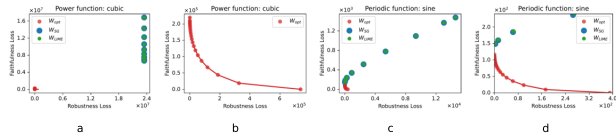


Figure 3: Comparison of Faithfulness and Robustness losses evaluated at  $W_{opt}$  (RBF Kernel) vs  $W_{SG}$  and  $W_{LIME}$  (Normal Sampling). The losses for  $W_{opt}$  are red,  $W_{SG}$  are blue and  $W_{LIME}$  are green. Functions are  $\sum_{d=1}^D x_d^3$ ,  $\sum_{d=1}^D sin(x^{(d)})$

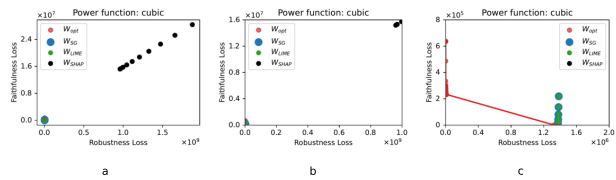


Figure 4: Comparison of Faithfulness and Robustness losses evaluated at  $W_{opt}$  (RBF Kernel) vs  $W_{SG}$ ,  $W_{LIME}$  and  $W_{SHAP}$  (Normal Sampling) for  $\sum_{d=1}^D x_d^3$ .

SHAP and we noticed that evaluating the faithfulness and robustness loss for SHAP is unreasonable as it provides explanations using a game theoretic approach to compute feature importance’s. As a result, the losses for SHAP look unreasonable when compared to LIME, SmoothGrad and our method as shown in figure4. To show that we zoomed into the figure twice in 4b and 4c.

**Inductive Setting.** In Figure 5, we show that inductive solutions approach transductive solutions exponentially fast as the number of inducing points are increased. This means the benefits we have seen so far can be achieved in the inductive setting as well (although for a more restricted set of properties).

Finally, we also provide a visual example to emphasize our main argument: Directly optimizing for desired properties allow us to manage a wide range of trade-offs between properties. Without an explicit optimization step, existing methods offer limited range of control. In Figure 6, we generate explanations for an image with both our approach and SmoothGrad. Our approach achieves arbitrary balance between faithfulness, robustness, and smoothness. Meanwhile, the hyperparameter  $\delta$  of SmoothGrad only provides control over the faithfulness vs. robustness trade-off and SmoothGrad never optimizes for smoothness (despite the fact

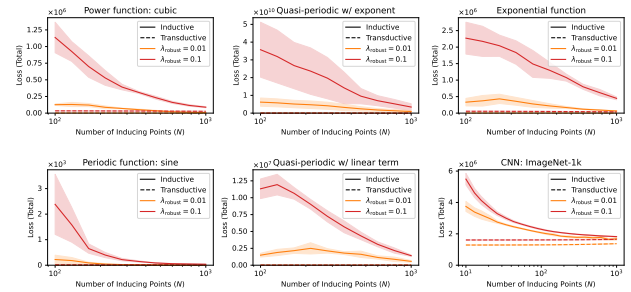


Figure 5: As the number of inducing points increases, inductive solutions obtained via GP inference (optimizing faithfulness and robustness) approach to transductive solutions on an exponential scale.

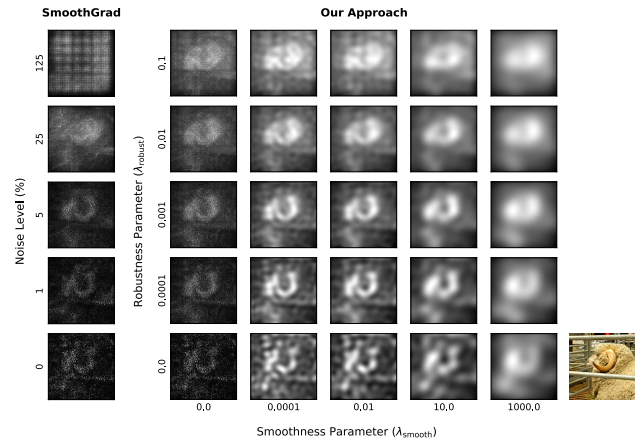


Figure 6: Our approach can achieve an arbitrary balance between faithfulness, robustness, and smoothness. Meanwhile, SmoothGrad can only manage the trade-off between faithfulness and robustness, and does not optimize for smoothness.

SmoothGrad aims to obtain smooth explanations).

## 8 CONCLUSION

A growing number of studies show that different downstream applications may require explanation with different properties. Yet existing feature attribution methods like SmoothGrad and LIME neither directly optimize for arbitrary explanation properties, nor can they manage trade-off between properties that are in tension.

In our work, we introduced a framework that can efficiently optimize for a set of desired explanation properties. In addition, our framework can also explicitly and intuitively manage trade-off between properties through our hyperparameters. We address settings in which we have the entire dataset (transductive) as well as settings in which we must generalize our property-optimized explanations to unseen data (inductive).

## References

Solar Flare. UCI Machine Learning Repository, 1989. DOI: <https://doi.org/10.24432/C5530G>.

- Iranian Churn. UCI Machine Learning Repository, 2020. DOI: <https://doi.org/10.24432/C5JW3Z>.
- Julius Adebayo, Justin Gilmer, Michael Muelly, Ian Goodfellow, Moritz Hardt, and Been Kim. Sanity Checks for Saliency Maps. In *Advances in Neural Information Processing Systems*, volume 31. Curran Associates, Inc., 2018. URL [https://papers.nips.cc/paper\\_files/paper/2018/hash/294a8ed24b1ad22ec2e7efea049b8737-Abstract.html](https://papers.nips.cc/paper_files/paper/2018/hash/294a8ed24b1ad22ec2e7efea049b8737-Abstract.html).
- David Alvarez Melis and Tommi Jaakkola. Towards robust interpretability with self-explaining neural networks. *Advances in neural information processing systems*, 31, 2018a.
- David Alvarez Melis and Tommi Jaakkola. Towards Robust Interpretability with Self-Explaining Neural Networks. In *Advances in Neural Information Processing Systems*, volume 31. Curran Associates, Inc., 2018b. URL [https://proceedings.neurips.cc/paper\\_files/paper/2018/hash/3e9f0fc9b2f89e043bc6233994dfcf76-Abstract.html](https://proceedings.neurips.cc/paper_files/paper/2018/hash/3e9f0fc9b2f89e043bc6233994dfcf76-Abstract.html).
- David Alvarez-Melis and Tommi S. Jaakkola. On the Robustness of Interpretability Methods, June 2018. URL <http://arxiv.org/abs/1806.08049>. arXiv:1806.08049 [cs, stat].
- David Baehrens, Timon Schroeter, Stefan Harmeling, Motoaki Kawanabe, Katja Hansen, and Klaus-Robert Müller. How to explain individual classification decisions. *The Journal of Machine Learning Research*, 11:1803–1831, 2010.
- Aparna Balagopalan, Haoran Zhang, Kimia Hamidieh, Thomas Hartvigsen, Frank Rudzicz, and Marzyeh Ghassemi. The road to explainability is paved with bias: Measuring the fairness of explanations. In *Proceedings of the 2022 ACM Conference on Fairness, Accountability, and Transparency*, pages 1194–1206, 2022.
- Naman Bansal, Chirag Agarwal, and Anh Nguyen. Sam: The sensitivity of attribution methods to hyperparameters. In *Proceedings of the IEEE/CVF Conference on Computer Vision and Pattern Recognition*, pages 8673–8683, 2020.
- Umang Bhatt, Adrian Weller, and José M. F. Moura. Evaluating and Aggregating Feature-based Model Explanations. In *Proceedings of the Twenty-Ninth International Joint Conference on Artificial Intelligence*, pages 3016–3022, Yokohama, Japan, July 2020. International Joint Conferences on Artificial Intelligence Organization. ISBN 978-0-9992411-6-5. doi: 10.24963/ijcai.2020/417. URL <https://www.ijcai.org/proceedings/2020/417>.
- Zixi Chen, Varshini Subhash, Marton Havasi, Weiwei Pan, and Finale Doshi-Velez. What Makes a Good Explanation?: A Harmonized View of Properties of Explanations, December 2022. URL <http://arxiv.org/abs/2211.05667>. arXiv:2211.05667 [cs].
- Julien Colin, Thomas Fel, Rémi Cadène, and Thomas Serre. What i cannot predict, i do not understand: A human-centered evaluation framework for explainability methods. *Advances in neural information processing systems*, 35:2832–2845, 2022.
- Paulo Cortez, A. Cerdeira, F. Almeida, T. Matos, and J. Reis. Wine quality. UCI Machine Learning Repository, 2009. DOI: <https://doi.org/10.24432/C56S3T>.
- Robin Cugny, Julien Aligon, Max Chevalier, Geoffrey Roman Jimenez, and Olivier Teste. AutoXAI: A Framework to Automatically Select the Most Adapted XAI Solution. In *Proceedings of the 31st ACM International Conference on Information & Knowledge Management*, pages 315–324, Atlanta GA USA, October 2022. ACM. ISBN 978-1-4503-9236-5. doi: 10.1145/3511808.3557247. URL <https://dl.acm.org/doi/10.1145/3511808.3557247>.
- Thomas Decker, Ananta R Bhattarai, Jindong Gu, Volker Tresp, and Florian Buettner. Provably better explanations with optimized aggregation of feature attributions. *arXiv preprint arXiv:2406.05090*, 2024.
- Amirata Ghorbani, Abubakar Abid, and James Zou. Interpretation of Neural Networks is Fragile, November 2018. URL <http://arxiv.org/abs/1710.10547>. arXiv:1710.10547 [cs, stat].
- Kaiming He, Xiangyu Zhang, Shaoqing Ren, and Jian Sun. Deep residual learning for image recognition. In *Proceedings of the IEEE conference on computer vision and pattern recognition*, pages 770–778, 2016.
- Q. Vera Liao, Yunfeng Zhang, Ronny Luss, Finale Doshi-Velez, and Amit Dhurandhar. Connecting Algorithmic Research and Usage Contexts: A Perspective of Contextualized Evaluation for Explainable AI. *Proceedings of the AAAI Conference on Human Computation and Crowdsourcing*, 10:147–159, October 2022. ISSN 2769-1349. doi: 10.1609/hcomp.v10i1.21995. URL <https://ojs.aaai.org/index.php/HCOMP/article/view/21995>.
- Scott M Lundberg and Su-In Lee. A Unified Approach to Interpreting Model Predictions. In *Advances in Neural Information Processing Systems*, volume 30. Curran Associates, Inc., 2017. URL [https://proceedings.neurips.cc/paper\\_files/paper/2017/hash/8a20a8621978632d76c43dfd28b67767-Abstract.html](https://proceedings.neurips.cc/paper_files/paper/2017/hash/8a20a8621978632d76c43dfd28b67767-Abstract.html).
- Eura Nofshin, Esther Brown, Brian Lim, Weiwei Pan, and Finale Doshi-Velez. A Sim2Real Approach for

- Identifying Task-Relevant Properties in Interpretable Machine Learning, May 2024. URL <http://arxiv.org/abs/2406.00116>. arXiv:2406.00116 [cs].
- Marco Tulio Ribeiro, Sameer Singh, and Carlos Guestrin. "Why Should I Trust You?": Explaining the Predictions of Any Classifier, August 2016. URL <http://arxiv.org/abs/1602.04938>. arXiv:1602.04938 [cs, stat].
- Olga Russakovsky, Jia Deng, Hao Su, Jonathan Krause, Sanjeev Satheesh, Sean Ma, Zhiheng Huang, Andrej Karpathy, Aditya Khosla, Michael Bernstein, Alexander C. Berg, and Li Fei-Fei. ImageNet Large Scale Visual Recognition Challenge. *International Journal of Computer Vision (IJCV)*, 115(3):211–252, 2015. doi: 10.1007/s11263-015-0816-y.
- Mark Schmidt. Least squares optimization with  $l_1$ -norm regularization. *CS542B Project Report*, 504 (2005):195–221, 2005.
- Ramprasaath R. Selvaraju, Michael Cogswell, Abhishek Das, Ramakrishna Vedantam, Devi Parikh, and Dhruv Batra. Grad-CAM: Visual Explanations from Deep Networks via Gradient-based Localization. *International Journal of Computer Vision*, 128 (2):336–359, February 2020. ISSN 0920-5691, 1573-1405. doi: 10.1007/s11263-019-01228-7. URL <http://arxiv.org/abs/1610.02391>. arXiv:1610.02391 [cs].
- Karen Simonyan. Deep inside convolutional networks: Visualising image classification models and saliency maps. *arXiv preprint arXiv:1312.6034*, 2013.
- Dylan Slack, Sophie Hilgard, Emily Jia, Sameer Singh, and Himabindu Lakkaraju. Fooling LIME and SHAP: Adversarial Attacks on Post hoc Explanation Methods, February 2020. URL <http://arxiv.org/abs/1911.02508>. arXiv:1911.02508 [cs, stat].
- Daniel Smilkov, Nikhil Thorat, Been Kim, Fernanda Viégas, and Martin Wattenberg. SmoothGrad: removing noise by adding noise, June 2017. URL <http://arxiv.org/abs/1706.03825>. arXiv:1706.03825 [cs, stat].
- Zeren Tan and Yang Tian. Robust explanation for free or at the cost of faithfulness. In *International Conference on Machine Learning*, pages 33534–33562. PMLR, 2023a.
- Zeren Tan and Yang Tian. Robust Explanation for Free or At the Cost of Faithfulness. In *Proceedings of the 40th International Conference on Machine Learning*, pages 33534–33562. PMLR, July 2023b. URL <https://proceedings.mlr.press/v202/tan23a.html>. ISSN: 2640-3498.
- Zifan Wang, Haofan Wang, Shakul Ramkumar, Piotr Mardziel, Matt Fredrikson, and Anupam Datta. Smoothed geometry for robust attribution. *Advances in neural information processing systems*, 33:13623–13634, 2020.
- Chih-Kuan Yeh, Cheng-Yu Hsieh, Arun Suggala, David I Inouye, and Pradeep K Ravikumar. On the (in) fidelity and sensitivity of explanations. *Advances in neural information processing systems*, 32, 2019a.
- Chih-Kuan Yeh, Cheng-Yu Hsieh, Arun Suggala, David I Inouye, and Pradeep K Ravikumar. On the (In)fidelity and Sensitivity of Explanations. In *Advances in Neural Information Processing Systems*, volume 32. Curran Associates, Inc., 2019b. URL [https://proceedings.neurips.cc/paper\\_files/paper/2019/hash/a7471fdc77b3435276507cc8f2dc2569-Abstract.html](https://proceedings.neurips.cc/paper_files/paper/2019/hash/a7471fdc77b3435276507cc8f2dc2569-Abstract.html).
- Jianlong Zhou, Amir H. Gandomi, Fang Chen, and Andreas Holzinger. Evaluating the Quality of Machine Learning Explanations: A Survey on Methods and Metrics. *Electronics*, 10(5):593, January 2021. ISSN 2079-9292. doi: 10.3390/electronics10050593. URL <https://www.mdpi.com/2079-9292/10/5/593>. Number: 5 Publisher: Multidisciplinary Digital Publishing Institute.

# Directly Optimizing Explanations for Desired Properties: Supplementary Materials

---

## A CHOICE OF SIMILARITY FUNCTION

In the above, we need to choose a similarity function  $s(\mathbf{x}, \mathbf{x}')$ . Certain similarity functions lend themselves to more efficient optimization. In particular, in the subsequent section, we show that when  $s(\mathbf{x}, \mathbf{x}') = -k^{-1}(\mathbf{x}, \mathbf{x}')$  is the precision of a kernel function  $k$ , optimization in the inductive setting becomes equivalent to Gaussian process inference. As examples, in this work, we consider similarity measures that are induced by the following two kernels: (i)  $k_{\text{threshold}}(\mathbf{x}, \mathbf{x}'; \Lambda) = \mathbb{1}\{\|\mathbf{x} - \mathbf{x}'\|_2^2 \leq \Lambda\}$  and (ii)  $k_{\text{gaussian}}(\mathbf{x}, \mathbf{x}'; \Lambda) = \exp\{-\|\mathbf{x} - \mathbf{x}'\|_2^2/2\Lambda^2\}$ . In practice, we note that the choice of  $s$  or an associated kernel  $k$  should be informed by domain knowledge (e.g. capture a notion of similarity between inputs that is meaningful for the user’s downstream task).

## B BACKGROUND ON EXISTING EXPLANATION METHODS

We compare our method, of directly optimizing explanations for properties, to three popular baseline methods for generating explanations: SmoothGrad Smilkov et al. (2017), LIME Ribeiro et al. (2016), and SHAP Lundberg and Lee (2017). All of these methods rely on point-wise local perturbations. We define a local perturbation of  $\mathbf{x}_n$  as  $\tilde{\mathbf{x}}_{n,s} = \mathbf{x}_n + \epsilon_s$ , where the noise  $\epsilon_s \in \mathbb{R}^D$  is sampled from some perturbation distribution  $p(\epsilon)$ . In this work, we consider two sampling distributions for the noise  $\epsilon_s$ : a zero-mean Gaussian  $\mathcal{N}(\mathbf{0}, \delta^2 \mathbf{I})$ , and a uniform distribution  $\text{Uniform}(B_{\delta^2})$ , where  $B_{\delta^2}$  is the ball of radius  $\delta^2$  in  $\mathbb{R}^D$  centered at the origin.

SmoothGrad is defined as the average of the gradients of  $f$  in a neighbourhood of  $\mathbf{x}_n$ . Typically, SmoothGrad is computed by sampling points in this neighbourhood, where the sampling hyperparameter  $\delta_{SG}$  controls the size of the neighbourhood:

$$W_{SG_n} = \frac{1}{S} \sum_{s=1}^S \nabla f(\tilde{\mathbf{x}}_{n,s}) \tag{17}$$

Intuitively, the sampling size parameter  $\delta_{SG}$  controls the degree of smoothing applied to  $W_{SG_n}$ . In the original formulation of SmoothGrad, the sampling distribution is Gaussian. Later, the authors of Wang et al. (2020), introduces UniGrad, where the sampling distribution is uniform over an interval. In this work, we denote both methods as SmoothGrad and explicitly describe the sampling distribution.

LIME approximates  $f$  at  $\mathbf{x}_n$  with a linear model trained on a set of points sampled from a  $\delta_{LIME}$ -neighbourhood of  $\mathbf{x}_n$ :

$$\begin{aligned} W_{LIME_n} &= \underset{\mathbf{w}}{\text{argmin}} \sum_{s=1}^S (f(\tilde{\mathbf{x}}_{n,s}) - g(\tilde{\mathbf{x}}_{n,s}, \mathbf{w}))^2 \mathbf{K}_{n,n'} \end{aligned} \tag{18}$$

where  $k_{n,n'} = k(x_n, x'_n)$  for a kernel function  $k$ , and  $g$  is a weighted linear model  $g(\tilde{\mathbf{x}}_{n,s}, \mathbf{w}) = \mathbf{w}^T(\tilde{\mathbf{x}}_{n,s})$ . Note that the LIME objective function can include an optional regularizer. The sampling hyperparameter  $\delta_{LIME}$  controls the size of the neighbourhood. As  $\delta_{LIME}$  approaches zero,  $W_{LIME,n}$  approaches the local gradient  $\nabla f(\mathbf{x}_n)$ .

## C PROOF OF PROPOSITION 1

For a sufficiently large  $N$ , the objective in Equation 8 can be written as:

$$\operatorname{argmin}_E \sum_n \|E(\mathbf{x}_n) - \nabla f(\mathbf{x}_n)\|_2^2 - \sum_{n,n',d,d'} |E_d(\mathbf{x}_n) - E_{d'}(\mathbf{x}_{n'})|^2 K_{dd'}^{-1}(\mathbf{x}_n, \mathbf{x}'_n) \quad (19)$$

We show that, as  $N \rightarrow \infty$  and  $\sigma^2 \rightarrow \infty$ , maximizing  $\log p(E|\{\mathbf{x}_n, \nabla f(\mathbf{x}_n)\})$  becomes equivalent to this objective.

For simplicity, we switch to a vectorized notation so that we can work with a single-dimensional GP:  $\mathbf{E} = [E(\mathbf{x}_1) \dots E(\mathbf{x}_N)] \in \mathbb{R}^{ND}$ ,  $\nabla \mathbf{f} = [\nabla f(\mathbf{x}_1) \dots \nabla f(\mathbf{x}_N)] \in \mathbb{R}^{ND}$ , and

$$\mathbf{K} = \begin{bmatrix} K(\mathbf{x}_1, \mathbf{x}_1) & \dots & K(\mathbf{x}_1, \mathbf{x}_N) \\ \vdots & \ddots & \vdots \\ K(\mathbf{x}_N, \mathbf{x}_1) & \dots & K(\mathbf{x}_N, \mathbf{x}_N) \end{bmatrix} \in \mathbb{R}^{ND \times ND} \quad (20)$$

Let us first consider only the prior term in the GP, marginalizing out the random mean explanation  $\mu$  from the joint distribution:

$$p(\mathbf{E}, \mu) = p(\mathbf{E}|\mu)p(\mu) \propto \exp\left\{-\frac{1}{2}(\mathbf{E} - \mu \mathbf{1}_{ND})^\top \mathbf{K}^{-1}(\mathbf{E} - \mu \mathbf{1}_{ND})\right\} \exp\left\{-\frac{1}{2} \cdot \frac{\mu^2}{\sigma^2}\right\} \quad (21)$$

where  $\mathbf{1}_{ND} \in \mathbb{R}^{ND}$  is a vector of ones (written as  $\mathbf{1}$  henceforth). By marginalizing out  $\mu$  in Equation 21 (after completing the square, followed by some algebra), we obtain  $p(\mathbf{E})$  as the following Gaussian:

$$p(\mathbf{E}) \propto \exp\left\{-\frac{1}{2} \mathbf{E}^\top \left( \underbrace{\mathbf{K}^{-1} - \frac{\mathbf{K}^{-1} \mathbf{1} \mathbf{1}^\top \mathbf{K}^{-1}}{\mathbf{1}^\top \mathbf{K}^{-1} \mathbf{1} + 1/\sigma^2}}_{\doteq \Sigma^{-1}} \right) \mathbf{E}\right\} \quad (22)$$

We denote the covariance of  $p(\mathbf{E})$  by  $\Sigma$ . This marginalization can be interpreted as a new Gaussian prior on the explanations  $\mathbf{E}$ ; we will still have a multivariate Gaussian—and associated GP—with this new kernel.

Next, we note that the posterior mean of multivariate Gaussian  $p(\mathbf{E}|\nabla \mathbf{f})$  is the solution to the least square regression problem, regularized by the precision matrix  $\Sigma^{-1}$  of the prior  $p(\mathbf{E})$  that we just derived above in Equation 22:

$$\max_{\mathbf{E}} \log p(\mathbf{E}|\nabla \mathbf{f}) \equiv \min_{\mathbf{E}} (\mathbf{E} - \nabla \mathbf{f})^\top (\mathbf{E} - \nabla \mathbf{f}) + \mathbf{E}^\top \Sigma^{-1} \mathbf{E} \quad (23)$$

With a little algebraic manipulation, the regularization term  $\mathbf{E}^\top \Sigma^{-1} \mathbf{E}$  can be further expanded as follows:

$$\mathbf{E}^\top \Sigma^{-1} \mathbf{E} = \underbrace{-\frac{1}{2} \sum_{\ell=1}^{ND} \sum_{\ell'=1}^{ND} |\mathbf{E}_\ell - \mathbf{E}_{\ell'}|^2 \Sigma_{\ell\ell'}^{-1}}_{\text{Term 1}} + \underbrace{\sum_{\ell=1}^{ND} \left( |\mathbf{E}_\ell|^2 \sum_{\ell'=1}^{ND} \Sigma_{\ell\ell'}^{-1} \right)}_{\text{Term 2}} \quad (24)$$

We first observe that the second term goes to zero as the variance of the explanation mean  $\sigma^2$  goes to infinity. Specifically, Term 2 in Equation 24 can be expanded as:

$$\sum_{\ell} |\mathbf{E}_\ell|^2 \left( \delta_\ell^\top \mathbf{K}_\ell^{-1} \mathbf{1} - \delta_\ell^\top \mathbf{K}_\ell^{-1} \mathbf{1} \left( \frac{\mathbf{1}^\top \mathbf{K}^{-1} \mathbf{1}}{\mathbf{1}^\top \mathbf{K}^{-1} \mathbf{1} + 1/\sigma^2} \right) \right) \quad (25)$$

where  $\delta_\ell$  is a vector of zeros except for the  $\ell$ -th element, which is one. As  $\sigma^2$  goes to infinity (representing an improper, uninformative prior over the value of the mean explanation), the fraction goes to one and the first and second terms in the kernel expression cancel.

Thus, we are left with only the first term:

$$\mathbf{E}^\top \Sigma^{-1} \mathbf{E} \approx \underbrace{-\frac{1}{2} \sum_{\ell=1}^{ND} \sum_{\ell'=1}^{ND} |\mathbf{E}_\ell - \mathbf{E}_{\ell'}|^2 \Sigma_{\ell\ell'}^{-1}}_{\text{Term 1}} \quad (26)$$

We are going to finish our proof by showing that  $\Sigma^{-1}$  tends to  $\mathbf{K}^{-1}$  as  $\sigma^2 \rightarrow \infty$  and  $N \rightarrow \infty$ . Let  $r = \mathbf{K}\mathbf{1}$  and  $r' = \mathbf{K}^{-1}\mathbf{1}$  be the vector of row sums for  $\mathbf{K}$  and  $\mathbf{K}^{-1}$  respectively. Now, as  $\sigma^2 \rightarrow \infty$ , we can re-write  $\Sigma^{-1}$  as

$$\Sigma_{\ell\ell'}^{-1} = \mathbf{K}_{\ell\ell'}^{-1} - \frac{\delta_\ell^\top (\mathbf{K}^{-1}\mathbf{1})(\mathbf{K}^{-1}\mathbf{1})^\top \delta_{\ell'}}{\mathbf{1}^\top (\mathbf{K}^{-1}\mathbf{1}) + 1/\sigma^2} = \mathbf{K}_{\ell,\ell'}^{-1} - \frac{r'_\ell r'_{\ell'}}{\sum_s r'_s + 1/\sigma^2} \approx \mathbf{K}_{\ell\ell'}^{-1} - \frac{r'_\ell r'_{\ell'}}{\sum_s r'_s} \quad (27)$$

Note that, if  $r_{\text{lower}} \leq r_s \leq r_{\text{upper}}$  for all  $s$ , then  $1/r_{\text{upper}} \leq r'_s \leq 1/r_{\text{lower}}$  for all  $s$ . Letting

$$K_{\max} \doteq \max_{\mathbf{x}, \mathbf{x}', d, d'} K_{dd'}(\mathbf{x}, \mathbf{x}') \quad (28)$$

$$K_{\min} \doteq \min_{\mathbf{x}, d} K_{dd}(\mathbf{x}, \mathbf{x}) \quad (29)$$

we have  $K_{\min} \leq r_s \leq NDK_{\max}$  hence  $1/NDK_{\max} \leq r'_s \leq 1/K_{\min}$ . Using these bounds, we obtain

$$\frac{K_{\min}}{N^3 D^3 K_{\max}^2} \leq \frac{r'_\ell r'_{\ell'}}{\sum_s r'_s} \leq \frac{(1/\min_s r_s)^2}{ND(1/\max_s r_s)} = \frac{\max_s r_s/N}{N^2 D \cdot (\min_s r_s/N)^2} \quad (30)$$

The left-hand side goes to zero as  $N \rightarrow \infty$ . For the right-hand side, let

$$n[s] = \lceil s/D \rceil \in \{1, \dots, N\} \quad (31)$$

$$d[s] = (s \bmod D) + 1 \in \{1, \dots, D\} \quad (32)$$

be the original dimensions corresponding to the flattened dimension  $s \in \{1, \dots, ND\}$ . Then, for input points  $\mathbf{x}_n \sim \mathcal{P}$  that are i.i.d. and as  $N \rightarrow \infty$ , we have

$$\frac{r_s}{N} = \frac{1}{N} \sum_{s'} \mathbf{K}_{ss'} = \frac{1}{N} \sum_{n', d'} K_{d[s], d'}(\mathbf{x}_{n[s]}, \mathbf{x}_{n'}) \rightarrow \mathbb{E}_{\mathbf{x}' \sim \mathcal{P}} \left[ \sum_{d'} K_{d[s], d'}(\mathbf{x}_{n[s]}, \mathbf{x}') \right] \doteq \bar{K}_{d[s]}(\mathbf{x}_{n[s]}) \quad (33)$$

Note that  $\bar{K}_d(\mathbf{x})$  is a function independent of  $\{\mathbf{x}_n\}$  and  $N$  with maxima  $\bar{K}_{\max} = \max_{\mathbf{x}, d} \bar{K}_d(\mathbf{x})$  and minima  $\bar{K}_{\min} = \min_{\mathbf{x}, d} \bar{K}_d(\mathbf{x})$  independent of  $\{\mathbf{x}_n\}$  and  $N$  as well. For sufficiently large  $N$ , we have

$$\frac{\max_s r_s/N}{N^2 D \cdot (\min_s r_s/N)^2} \approx \frac{\max_s \bar{K}_{d[s]}(\mathbf{x}_{n[s]})}{N^2 D \cdot (\min_s \bar{K}_{d[s]}(\mathbf{x}_{n[s]})^2} \leq \frac{\bar{K}_{\max}}{N^2 D \bar{K}_{\min}^2} \approx 0 \quad (34)$$

## D ADDITIONAL TRANSDUCTIVE SETTING RESULTS: POLYNOMIALS AND PERIODIC FUNCTIONS

Below we have additional results for polynomials and periodic functions in 3, 5, and 7 dimensions. We show that our method consistently provides optimal explanations with options to manage the trade-off between faithfulness and robustness. In contrast LIME and SmoothGrad are either providing explanations that are less optimal or they do not provide options to manage trade off between properties. For three-dimensional inputs, we sampled 100 points from an equally spaced grid within the range  $[-5, 5]$ . For five- and seven-dimensional inputs, we uniformly sampled points from the same range.

Note: The following shows how the functions in the main text correspond to the functions in the appendix.

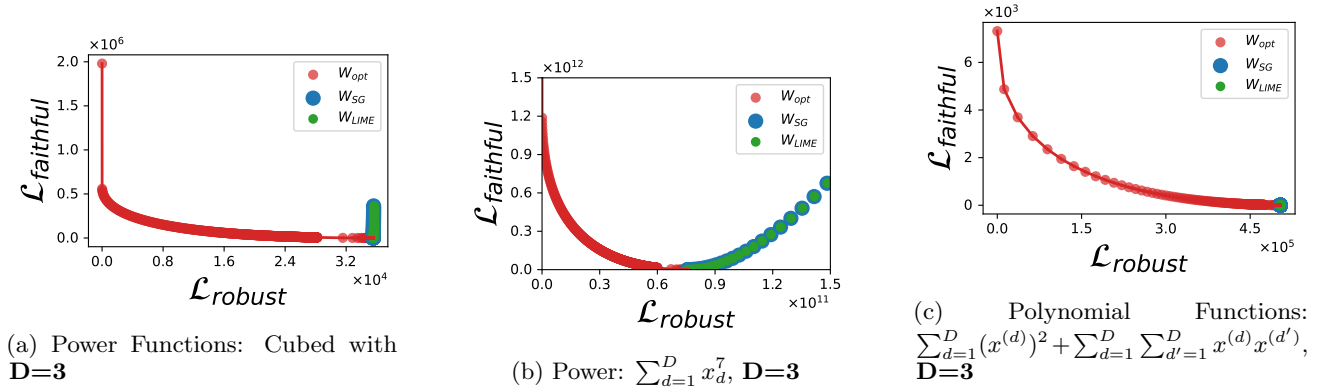
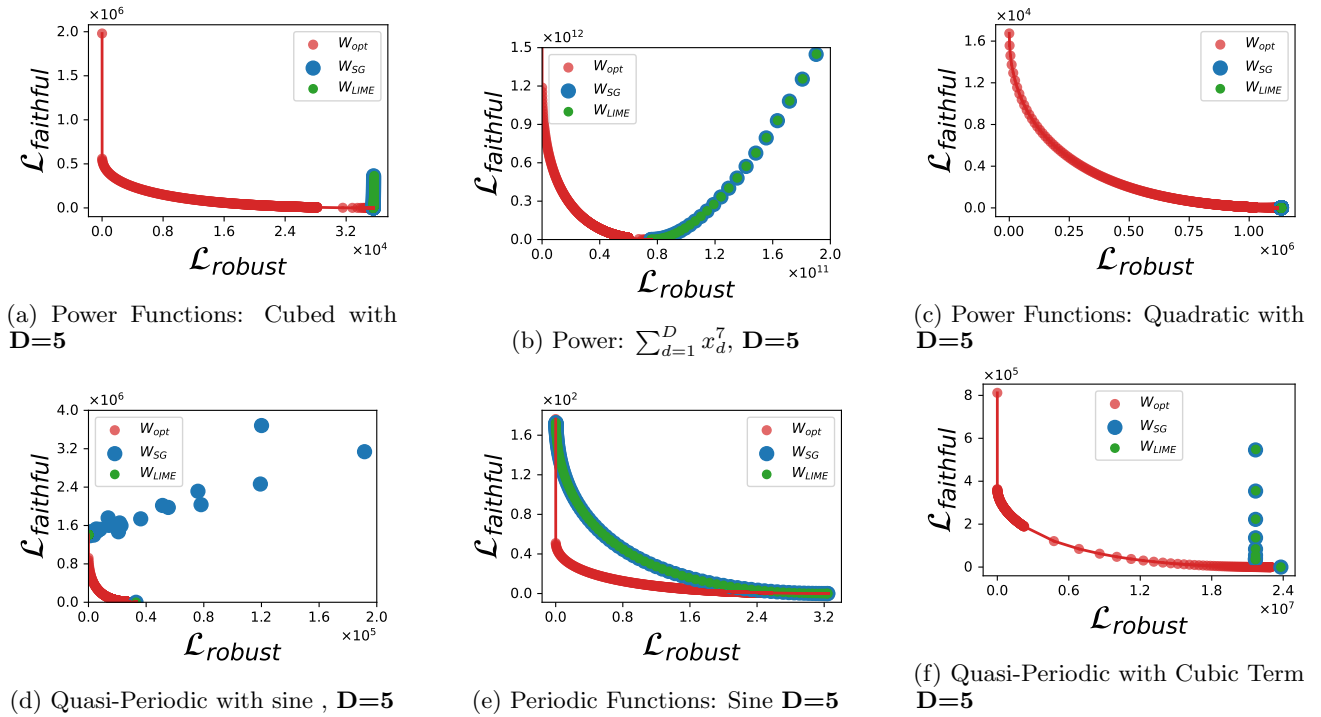
- Quasi-Periodic function 1- Quasi Periodic function with sine
- Quasi-Periodic function 2 - Quasi Periodic function with linear term
- Quasi-Periodic function 4 - Quasi Periodic function with quadratic term

### D.1 Trade-off between Faithfulness and Robustness for $D = 3$

In figure7 we used the faithfulness formalization defined in 2 and the robustness formalization defined in 3 for  $D = 3$

### D.2 Trade-off between Faithfulness and Robustness for $D = 5$

In figure8 we used the faithfulness formalization defined in 2 and the robustness formalization defined in 3 for  $D = 5$


 Figure 7: Faithfulness Vs. Robustness Trade-off for  $D=3$ 

 Figure 8: Faithfulness Vs. Robustness Trade-off for  $D=5$ 

### D.3 Trade-off between Faithfulness and Robustness for $D = 7$

In figure 9 we used the faithfulness formalization defined in 2 and the robustness formalization defined in 3 for  $D = 7$

### D.4 Trade-off Between Faithfulness (Gradient Matching Definition) and Robustness with Constraint for $D = 3$

In figure 10 we used the gradient matching faithfulness formalization defined in 2 and the robustness formalization defined in 13

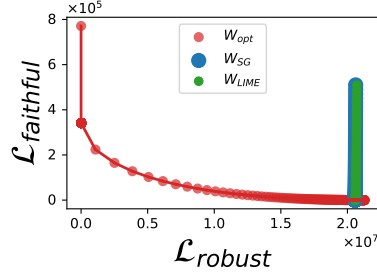
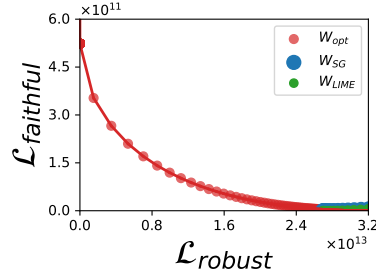
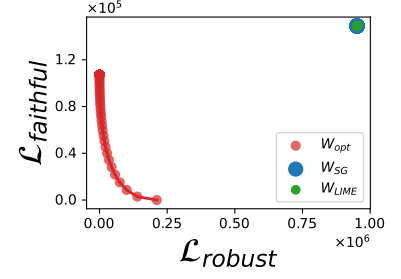

 (a) Power Functions: Cubed with  $D=7$ 

 (b) Power:  $\sum_{d=1}^D x_d^7$ ,  $D=7$ 

 (c) Power Functions: Quadratic with  $D=7$ 

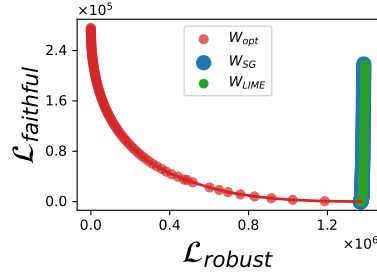
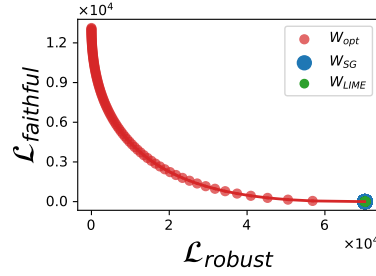
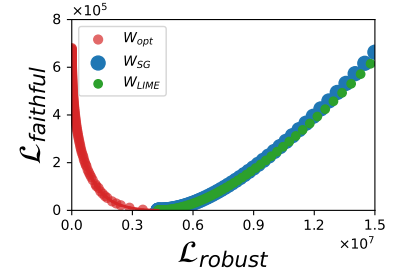
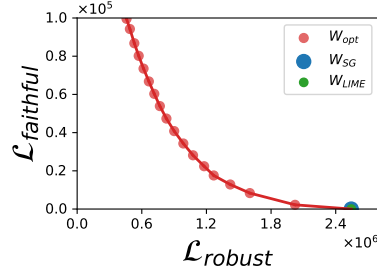
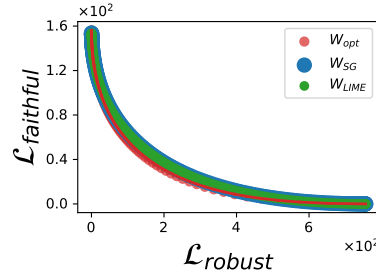
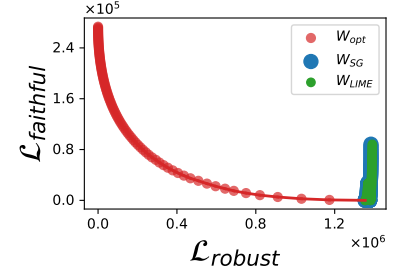
 Figure 9: Faithfulness Vs. Robustness Trade-off for  $D=7$ 

 (a) Power: Cubed with  $D=3$ 

 (b) Power: Quadratic  $D=3$ 

 (c) Exponential Function  $D=3$ 

 (d) Quasi-Periodic with Linear Term  $D=3$ 

 (e) Periodic: Sine  $D=3$ 

 (f) Quasi-Periodic with Cubic Term  $D=3$ 

 Figure 10: Faithfulness Vs. Robustness(Robustness with Constraint) Trade-off for  $D=3$ 

## D.5 Trade-off between Faithfulness(Function matching definition) and Robustness(with out constraint) for $D=3$

In figure 11 For this set of experiments we used the function matching faithfulness formalization defined in 12 and the Robustness formalization defined in 3.

## E ADDITIONAL TRANSDUCTIVE SETTING RESULTS: MULTI-LAYER PERCEPTRONS

### E.1 Trade-off between Robustness and Faithfulness

We trained the neural network with two hidden layers using the following three datasets from the UCI Machine Learning Repository: sol (1989), Cortez et al. (2009), and ira (2020). The results show that our method provide optimal explanations(better faithfulness and robustness loss) than SmoothGrad and LIME. We used the gradient matching faithfulness 2 and robustness formalization defined in 3 to generate the plots in figure 12.

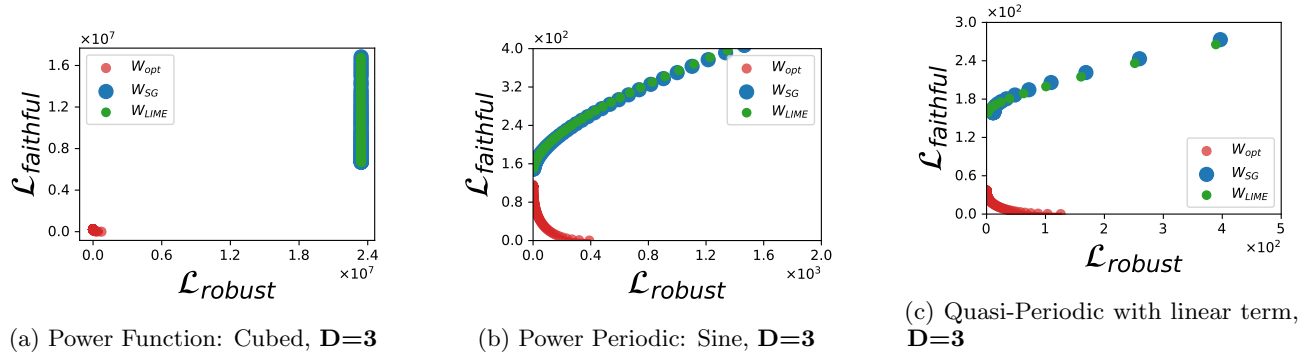
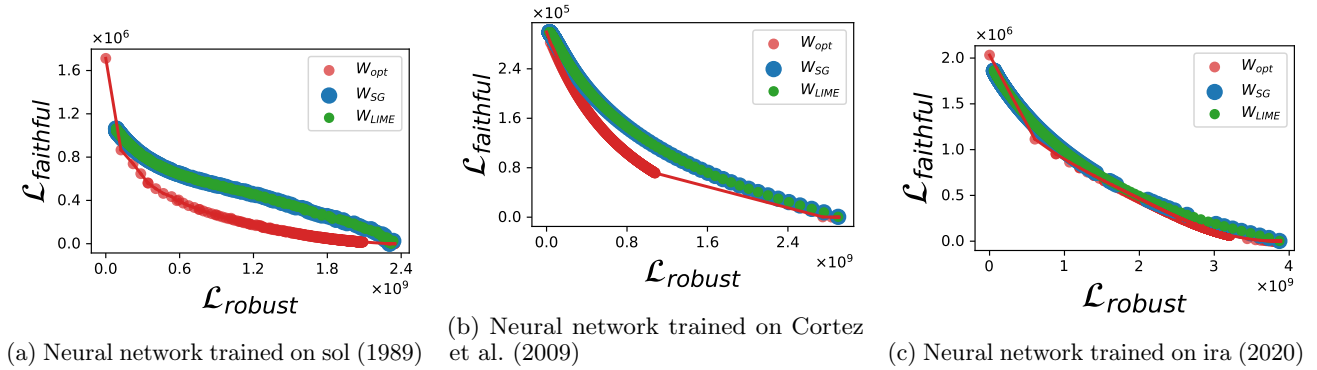

 Figure 11: Faithfulness (Function matching) Vs. Robustness with  $D=3$ 


Figure 12: Faithfulness Vs. Robustness Trade-off for Neural Networks

## F FURTHER QUALITATIVE EVALUATION

In Figure 6, we argued that our approach can control the balance between faithfulness, robustness and smoothness while highlighting that SmoothGrad can only manage the trade-off between faithfulness and robustness (missing smoothness). Here, we present a similar figure but for a different starting image (Figure 13) to show that this pattern is not limited to a single instance.

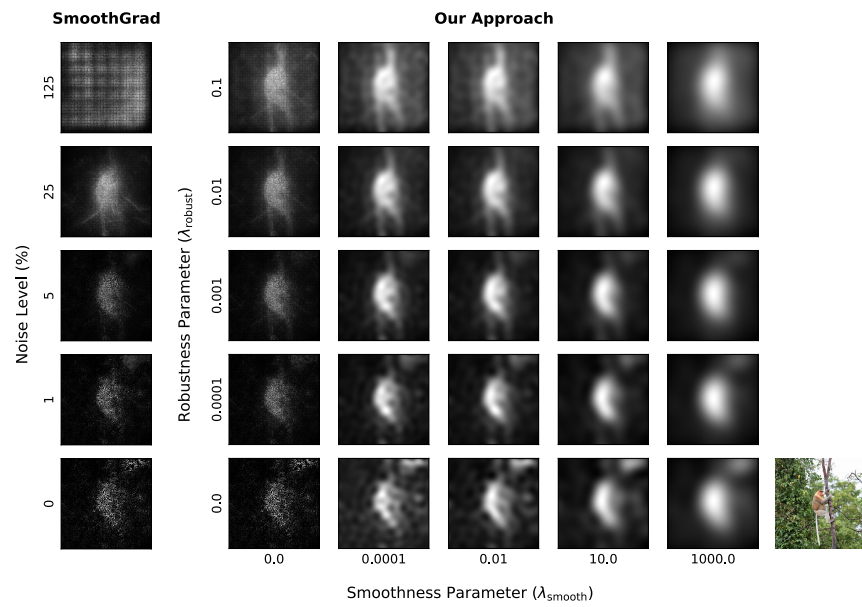


Figure 13: Comparison of our approach vs. SmoothGrad for a different input image when explaining image-based models.